Acta Pharmacologica Sinica

www.nature.com/aps

ARTICLE

Humanized cerebral organoids-based ischemic stroke model for discovering of potential anti-stroke agents

Shu-na Wang[1], Zhi Wang[1], Xi-yuan Wang[1], Xiu-ping Zhang[1], Tian-ying Xu[1,2] and Chao-yu Miao[1]

Establishing a stoke experimental model, which is better in line with the physiology and function of human brain, is the bottleneck for the development of effective anti-stroke drugs. A three-dimensional cerebral organoids (COs) from human pluripotent stem cells can mimic cell composition, cortical structure, brain neural connectivity and epigenetic genomics of in-vivo human brain, which provides a promising application in establishing humanized ischemic stroke model. COs have been used for modeling low oxygen condition-induced hypoxic injury, but there is no report on the changes of COs in response to in vitro oxygen-glucose deprivation (OGD)-induced damage of ischemic stroke as well as its application in testing anti-stroke drugs. In this study we compared the cell composition of COs at different culture time and explored the cell types, cell ratios and volume size of COs at 85 days (85 d-CO). The 85 d-CO with diameter more than 2 mm was chosen for establishing humanized ischemic stroke model of OGD. By determining the time-injury relationship of the model, we observed aggravated ischemic injury of COs with OGD exposure time, obtaining first-hand evidence for the damage degree of COs under different OGD condition. The sensitivity of the model to ischemic injury and related treatment was validated by the proven pan-Caspase inhibitor Z-VAD-FMK (20 μM) and Bcl-2 inhibitor navitoclax (0.5 μM). Neuroprotective agents edaravone, butylphthalide, P7C3-A20 and ZL006 (10 μM for each) exerted similar beneficial effects in this model. Taken together, this study establishes a humanized ischemic stroke model based on COs, and provides evidence as a new research platform for anti-stroke drug development.

Keywords: ischemic stroke; pluripotent stem cells; cerebral organoids; humanized model; neuroprotection

Acta Pharmacologica Sinica (2023) 44:513–523; https://doi.org/10.1038/s41401-022-00986-4

INTRODUCTION

Stroke is the second leading cause of death and third leading cause of disability in adults worldwide, with one in four people affected over their lifetime, but with few effective therapies [1, 2]. Despite the rate of incidence and mortality is stable or even declining over decades, the number of stroke patients and survivors, disability-adjusted life-years lost due to stroke, and stroke-related deaths are increasing [3, 4]. Tissue plasminogen activator (tPA) is the only drug approved by FDA for ischemic stroke and no drug is available for hemorrhagic stroke. And, only 3%–5% stroke patients can receive tPA treatment, due to the narrow therapeutic window, contraindications and complications. Hence, it is urgent to develop effective drugs for stroke treatment.

Numerous neuroprotective agents targeting excitotoxicity, oxidative and nitrosative stress, inflammation or others have been studied from bench to bedside in the past decades, but almost all of them are failed or still in the transition of bench to bedside [5]. Many factors are related to the extremely low success rate of anti-stroke drug development. One of the major factors is the species difference between the experimental and clinical research [6, 7]. It is well-known that anti-stroke neuroprotective agents in the laboratory are primarily studied in rodent models, rather than primate or humanized models, which will be inevitable to misguide the clinical efficacy to some extent. Compared with human beings, rodents belong to anencephalic animals with difference in brain anatomy and functional organization, which determine that they cannot fully mimic the physiological, pathological and anatomic features of human brain. Although whether the lissencephalic structure of brain has an impact on the efficacy of anti-stroke drugs is still under debate, it is certain that the difference of brain anatomy and functional organization can affect the infarct localization [8]. Besides, rodent brain has lower percentage of white matter as compared to human brain. The percentage of white matter in whole brain accounts for 60% in humans, 15% in rats, and 10% in mice [7]. And the ischemic damage degree of white matter not only plays a vital role in the prognosis of stroke outcome, but also is the major cause of hemiparesis in stroke.

Compared with rodents, non-human primate animals are the better research subject for anti-stroke drug development, which have similar genetic background with human beings. However, there are disadvantages for non-human primate stroke model [9]. Firstly, the price of non-human primate animals is relatively expensive. Secondly, the in-vivo stroke model of middle cerebral artery occlusion surgery in non-human primate requires more seasoned operational experience and skills. Thirdly, the equipment

[1]Department of Pharmacology, Second Military Medical University/Naval Medical University, Shanghai 200433, China and [2]Department of Anesthesia Pharmacology, Second Military Medical University/Naval Medical University, Shanghai 200433, China
Correspondence: Chao-yu Miao (cymiao@smmu.edu.cn) or Tian-ying Xu (xty7910@163.com)
These authors contributed equally: Shu-na Wang, Zhi Wang, Xi-yuan Wang

Received: 13 June 2022 Accepted: 19 August 2022
Published online: 13 September 2022

© The Author(s), under exclusive licence to Shanghai Institute of Materia Medica, Chinese Academy of Sciences and Chinese Pharmacological Society 2022 SPRINGER NATURE

for long-term monitoring of non-human primate not only takes up space, and also is expensive. More importantly, the extensive use of non-human primates is contrary to the welfare and ethical issues of experimental animals, which cannot provide enough data for the repeatability across different study subgroups. Thus, how to establish a stoke research model, that is better in line with the physiology and function of human brain, has been the bottleneck for effective anti-stroke drug development.

The recent developed method for generating three-dimensional (3D) cerebral organoids (COs) from human pluripotent stem cells provides a new sight for stroke research. The in-vitro cultured COs not only have advantages in diverse cell types (including but not limited to, neural progenitor cells/neural stem cells [NPCs/NSCs], neurons, and glia cells), easy accessibility of cell resource, enough cell number for drug screening (more than 10^6 cells for single CO at 55 days) [10], and 3D tissue structure (up to 4 mm in diameter) [11, 12], but also show detectable neural connectivity and brain functionality that can recapitulate features of in-vivo human brain development and maturation [11, 13–15]. Moreover, the cultured COs have similar cell composition, cortical structure and epigenetic genomics as compared to human brain [16]. The COs contain most neural lineage cells that are expressed in human brain, and especially have positive expression of outer radial glial cells that are not expressed in rodent brain [11]. And outer radial glial cells have a key role in the evolutionary expansion of the mammalian neocortex. Taken together, from the perspective for the drug development, the COs have a promising application in establishing humanized ischemic stroke model, and its unique features, such as high throughput, good accessibility and 3D complex structure, make them good alternatives to animal models for efficacy screening of potential anti-stroke drugs.

Although a most-recent study has subjected human COs to hypoxic injury to investigate neuronal damage and regeneration after hypoxic injury [17], the features of COs-based humanized ischemic stroke model in response to oxygen-glucose deprivation (OGD) damage and its application in testing anti-stroke drugs are still unknown. Our group have accumulated a series research experience in the development of potential anti-stroke drugs and in the study of NSCs and COs [10, 15, 18–22]. Therefore, this study is designed to establish humanized ischemic stroke model of OGD based on COs by exploring the cell type and composition of COs that is used for model preparation and the time-effect relationship of the model, and further verifying the feasibility and applicability of the model in potential anti-stroke drug efficacy testing, hoping to provide a novel platform for anti-stroke drug translational research.

MATERIALS AND METHODS

Human embryonic stem cell culture

Human embryonic stem cells (hESCs) H1 (passages 45–55) were cultured as previously described with minor modifications [22, 23]. In feeder-free mTesR™1 maintenance medium (STEMCELL, Vancouver, Canada) and hESC-qualified Matrigel (Corning, Corning, NY, USA) coated plates, hESCs were passaged at a ratio of 1:3 to 1:6 every 4–6 days. When digested into cell suspension by using TrypLE (Gibco, Carlsbad, CA, USA), the hESCs were collected and seeded in the Matrigel coated six-well tissue culture plates. And, 10 μM Y-27632 (Sigma-Aldrich, St. Louis, MO, USA) was added into mTesR™1 maintenance medium at the first day of passage. The use of hESCs in this study was complied with Ethical Guiding Principles for the Research of Human Embryonic Stem Cell.

Cerebral organoids culture

Cerebral organoids (COs) were generated as previously described [10, 12, 22]. When the cell confluence of hESCs was reached about 80%, single cell suspension (9×10^4 cells/mL) was prepared by Accutase (Gibco, Carlsbad, CA, USA) and seeded in the ultra-attachment 96-well plate (Corning, Corning, NY, USA) with low bFGF medium [DMEM/F12 (Invitrogen, Carlsbad, MA, USA) with 20% KoSR (Invitrogen, Carlsbad, CA, USA), 3% hES-quality FBS (Gibco, Carlsbad, CA, USA), 1% GlutaMAX (Invitrogen, Carlsbad, CA, USA), 1% MEM-NEAA (Invitrogen, Carlsbad, CA, USA), 55 μM 2-Mercaptoethanol (Sigma-Aldrich, St. Louis, MO, USA), 4 ng/mL bFGF (Peprotech, Rocky Hill, NJ, USA) and 50 μM Y-27632]. Twenty-four hours later, embryonic bodies (EBs) were formed, timing day 1. After 4–5 days, the diameter of single EBs was reached about 350 μm, and the culture medium was changed with hES medium (low bFGF medium without bFGF and Y-27632). After further 2–3 days, EBs grew larger with a diameter of 500 μm. Here, EBs were transferred into ultra-attachment 24-well plate with neural induction medium [DMEM-F12 with 1% N2 supplement (Invitrogen, Carlsbad, CA, USA), 1% GlutaMAX supplement, 1% MEM-NEAA and 1 μg/mL heparin solution (Sigma-Aldrich, St. Louis, MO, USA)] for 4–5 days. When radial organization of a pseudostratified epithelium was formed as an indicator of neuroepithelial bud formation in the plate, the neuroepithelial bud was embedded into Matrigel droplet with COs differentiation medium [50% DMEM/F12 and 50% Neurobasal medium with 0.5% N_2 supplement, 1% GlutaMAX supplement, 0.5% MEM-NEAA, 2.8 ng/mL human insulin solution (Sigma-Aldrich, St. Louis, MO, USA) and 1% B27 supplement without vitamin A] in a stationary culture condition. After 4–5 days, the cultured tissues were transferred into spinning bioreactor with COs maintenance medium [COs differentiation medium with 1 × B27 supplement (with vitamin A)] in Micro-Stir Slow Speed Magnetic Stirrers (Wheaton, Germany) at the speed of 85 rpm. Thereafter, the culture medium was changed every 4–7 days to support the growth, differentiation and maturation of COs.

Due to the heterogeneity of COs in morphology and size, we set strict selection criteria for COs that were used for this study. Firstly, parallel and consistent method for COs culture was strictly enforced as shown in above. Secondly, all COs used in the study were well identified with typical and qualified morphology in the different culture stage. And, the cell composition, cell type and cell number that indicated the growth, differentiation and maturation of COs in the different culture stage were examined.

Cryo-section and immunofluorescence staining of cerebral organoids

After fixation in 4% (wt/vol) PFA for 15 min and dehydration in 30% (wt/vol) sucrose solution at 4 °C overnight, COs were embedded into O.C.T. tissue freezing reagent (Leica, Heidelberg, Germany) and sectioned into cryosections (10 μm thickness) in the freezing microtome (Leica CM3050S, Heidelberg, Germany). In the process of immunofluorescence staining, 10% normal donkey serum (Jackson Immuno Research, West Grove, PA, USA) was used to block non-specific binding sites for 2 h at room temperature. Then, the slice was incubated with primary antibodies (Table 1) at 4 °C overnight. After washing by 1 × PBS, the slice was incubated with corresponding secondary antibodies (Alexa 488/594-conjugated, Table 1) for 2 h at room temperature under dark condition. And cell nuclei were stained with DAPI for 10 min at room temperature. The confocal laser scanning microscope (Olympus FV1000, Japan) was used to capture images. The quantitation of positive expression of immunostaining was counted by ImageJ 1.5 software (NIH, Bethesda, MD, USA, USA).

Flow cytometry

Single cell suspensions of COs were harvested by gentle cell dissociation reagent (STEMCELL, Vancouver, Canada). For cell surface flow cytometry staining, the cells were blocked with Fc Receptor Blocking Solution human TruStain FcX™ (BioLegend, San Diego, CA, USA) for 10 min, and then incubated with specific fluorescence-labeled antibodies (Table 1). For intracellular and cytoplasmic staining, the cells should be fixed and permeabilized by fixation buffer (BioLegend, San Diego, CA, USA) and

Table 1. Antibodies used in this study.

Antibodies	Cat. No.
SOX2	Abcam (ab97959)
Nestin	Abcam (ab6142)
Tuj1	Cell Signaling Technology (5568s) Abcam (ab78078) Abcam (ab7751)
NeuN	Abcam (ab177487)
GFAP	Abcam (ab7260)
Foxg1	Abcam (ab18259)
TTR	Abcam (ab9015)
VGAT	Santa Cruz (sc-393373)
VGlut	Abcam (ab227805)
BRN2	Santa Cruz (sc-393324)
POMC	Abcam (ab254257)
Calretin	Abcam (ab92341)
PSD-95	Cell Signaling Technology (2507s)
synaptophysin	Abcam (ab52636)
Cleaved-Caspase3	Cell Signaling Technology (9661S)
LC3B	Abcam (ab192890)
Phospho-RIP3	Abcam (ab195117)
GPX4	Abcam (ab125066)
FITC anti-human CD45 Antibody	Biolegend (304006)
PE anti-SOX2 Antibody	Biolegend (656104)
Alexa Fluor® 647 anti-Tuj1 Antibody	Biolegend (801210)
PE anti-Nestin Antibody	Biolegend (656806)
eFluor 660 anti-GFAP Antibody	eBioscience (50-9892-80)
Alexa Fluor® 594 Goat anti-Rabbit Secondary Antibody	Jackson (111-585-144)
Alexa Fluor® 488 Donkey anti-Mouse Secondary Antibody	Invitrogen (A-21202)
Alexa Fluor® 594 Donkey anti-Sheep Secondary Antibody	Abcam (ab150180)

intracellular staining permeabilization wash buffer (BioLegend, San Diego, CA, USA) successively. Then, the cells were incubated with specific fluorescence-labeled antibodies (Table 1) prepared by intracellular staining permeabilization wash buffer for 20 min. After setting compensation and quadrant markers based on blocking controls, isotype controls and unstained cells, all samples went proper flow cytometric analysis in BD FACS Calibur (BD, Franklin Lakes, NJ, USA).

Oxygen-glucose deprivation model

Oxygen-glucose deprivation (OGD) condition was prepared as described previously [24]. For the OGD model, COs were replenished with glucose-free Earle's balanced salt solution (EBSS) after washing by 1 × PBS, and incubated in the oxygen controllable CO_2 incubator (95% N_2, 5% CO_2, ≤1% O_2, 37 °C, Thermo Scientific, Carlsbad, CA, USA). For the control group, COs were cultured in the normal CO_2 incubator (5% CO_2, 37 °C) with EBSS containing glucose (25 mM). After OGD exposure ended, COs in the normal or OGD condition were taken out immediately for the following experimental testing.

Compound preparation and treatment

Compounds Z-VAD-FMK (Topscience, Shanghai, China), navitoclax (Topscience, Shanghai, China), edaravone (Selleck, Shanghai, China), butylphthalide (Selleck, Shanghai, China), P7C3-A20 (Shanghai Technology Yi Biotechnology Co. Ltd, Shanghai, China) and ZL006 (Sigma-Aldrich, St. Louis, MO, USA) were prepared in DMSO. The final concentration of 20 μM Z-VAD-FMK, 0.5 μM navitoclax, 10 μM edaravone, 10 μM butylphthalide, 10 μM P7C3-A20 and 10 μM ZL006 were given to COs during OGD exposure respectively. The final concentration of DMSO ≤ 0.1%.

Caspase 3 activity assay

Cell apoptosis was evaluated by Caspase 3 Activity Assay Kit (Beyotime, Shanghai, China) and Bradford Protein Assay Kit (Beyotime, Shanghai, China). Briefly, the protein concentration and Caspase 3 activity of each sample were detected by absorbance value ($OD_{595\,nm}$ and $OD_{405\,nm}$ respectively) in microplate reader (Tecan, Switzerland) according to the operating procedure. Caspase 3 activity per unit of protein concentration in each sample was used to indicate the degree of cell apoptosis.

LDH release assay

Cytotoxicity was evaluated by Cytotoxicity LDH Assay Kit-WST (Dojindo, Japan). According to the operating procedure, 100 μL culture supernatants were collected immediately into 96-well plate after experimental treatment, and incubated with 100 μL working solution. After 0–30 min incubation under dark condition, absorbance value ($OD_{490\,nm}$) was detected in the microplate reader (Tecan, Switzerland) to indicate the degree of cytotoxicity.

Immunohistochemistry staining

Immunohistochemistry staining was performed as previously described [22, 25]. After deparaffinating and rehydration, the paraffin-coated slice was soaked in citric acid buffer (pH 6.0) to enhance antigen exposure. Non-specific binding site was blocked by 8% donkey serum incubation for 2 h at room temperature. Then, the slice was incubated with primary antibodies (4 °C, overnight) (Table 1) and HRP-conjugated secondary antibody (room temperature, 2 h) sequentially. Then, fresh chromogenic substrate DAB was used to visualize the staining. Images were captured by digital microscope (Leica, Heidelberg, Germany). The quantitation of positive expression of immunostaining was counted by ImageJ 1.5 software.

Haematoxylin and eosin (HE) staining

COs in 4% paraformaldehyde were dehydrated with 30% sucrose in formalin (pH = 7.4), embedded in paraffin, and cut into slices (10 μm thickness). The slices were deparaffinized and stained with HE, and examined under a light microscope (Leica, Heidelberg, Germany).

Nissl's staining

Nissl's staining was performed as previous described [22]. After deparaffinating and rehydration, the paraffin-coated slice was incubated with toluidine blue and glacial acetic acid sequentially. After drying in the constant temperature oven, the slice was hyalinized with xylene. Images were captured by digital microscope. The quantitation of positive expression was counted by ImageJ 1.5 software.

Statistical analysis

Data were analyzed by using GraphPad Prism 8 software (GraphPad, San Diego, CA, USA). Statistical analyses were performed in the SPSS 11.0 software (SPSS Inc., Chicago, IL, USA). All data were presented as the normalized mean ± standard error of mean (SEM). Statistical differences were determined using two-tailed Student's *t* test in comparison between two groups. One-way ANOVA followed by post-hoc Tukey-Kramer tests was used in comparison among groups. P values < 0.05 were considered statistically significant.

RESULTS

The in-vitro culture and identification of cerebral organoids (COs)
As shown in Fig. 1a, hESCs underwent EB formation (Day 2), germ layer differentiation (Day 4), neuroectoderm induction (Day 9) in the low-attachment culture plate, and polarized neuroepithelium-like structures with characteristics of fluid-filled cavity in the Matrigel droplets (Day 14) successively. Then, the cultured tissues were transferred into the spinning bioreactor (Day 17) for further differentiation and maturation of COs. During the initial induction period, the EBs were gradually differentiated into NPCs/NSCs (SOX2 and Nestin, respectively), as shown in COs at 15 days (15 d-CO) (Fig. 1b). With the prolongation of induction time, the cultured COs gradually displayed positive expression of terminal differentiated neural cells (neurons, Tuj-1; astrocytes, GFAP) (Fig. 1b). And, expression of neurons and astrocytes in 75 d-CO was more than that in 35 d-CO (Fig. 1b), indicating continuously neural differentiation and maturation of in-vitro COs. Besides, 75 d-CO showed brain-region specific identities with positive expression of forebrain (Foxg1) and choroid plexus (TTR) (Fig. 1c), indicating the successful generation of COs. With further prolongation of culture time, the volume size of COs gradually increased and the center of the tissue may form apoptotic cavity structure due to insufficient nutrition. In order to explore whether there was formation of apoptotic cavity structure for the long-term cultured COs, we introduced apoptotic cell marker Cleaved-Caspase 3 and found the formation of apoptotic cavity in tissue center of 140 d-CO (Fig. 1d).

Choosing COs with culture time of about 85 days for establishing humanized ischemic stroke model
COs at different in-vitro culture time had different cell composition. The formation of brain-region specific forebrain (Foxg1) and choroid plexus (TTR) in 75 d-CO is an important characteristic for successful generation of relatively matured COs. Compared with 75 d-CO, the degree of cell differentiation and maturation in 85 d-CO further increased with positive expression NSCs (Nestin), neurons (Tuj-1), mature neurons (NeuN), astrocytes (GFAP), forebrain (Foxg1) and choroid plexus (TTR) (Fig. 2a). And the cell composition in 85 d-CO was mainly consisted of terminal neural cell types, including positive expression of inhibitory neurons (VGAT), excitatory glutamatergic neurons (VGlut), upper-layer neurons of cortical layers (BRN2), peptidergic neurons (POMC) and interneurons (Calretin) (Fig. 2a). Especially, many neurons in 85 d-CO had positive co-expression of presynaptic protein synaptophysin (Tuj1/SYN) and postsynaptic protein postsynaptic density 95 (Tuj1/PSD-95) (Fig. 2a), suggesting the higher cell maturation degree in 85 d-CO.

It is well-known that terminal neural cell types, especially neurons, are the main cell composition of ischemic damage in human brain. Further flow cytometry also demonstrated the main cell composition of neurons in 85 d-CO, as indicated 73.6% $Tuj1^+$ Neurons, 13.4% $GFAP^+$ astrocytes and 14.5% $Nestin^+$ NSCs in total (Fig. 2b1–3). Notably, the cell proportion of $SOX2^+$ cells was up to 21.2% (Fig. 2b4). It is well-known that SOX2 functions are critical for stem cells of embryonic, neural, and others to preserve stemness [26], and mediate the reprogramming of differentiated cells to stem cells [27]. However, in differentiated neurons, glia and other neural cell types, SOX2 is either not expressed, or important for very specific cell types. For example, a recent study reported SOX2 was strongly expressed in mouse postmitotic thalamic projection neurons [28]. Thus, the high cell proportion of $SOX2^+$ cells made us have to wonder whether there was $Tuj1^+$/$SOX2^+$ neurons in cultured 85 d-CO. Further flow cytometry confirmed our hypothesis and found there was about 16.3% $Tuj1^+$/SOX^+ cells in 85 d-CO, providing more evidence for the higher similarity between 85 d-CO and in-vivo brain (Fig. 2b5). Besides, we previously demonstrated that the cell number in single 85 d-CO was more than 2×10^6 cells [22], which also provides evidence for the enough cell number in single CO for drug efficacy testing. Moreover, many studies already demonstrated COs can faithfully model the gene expression, proteomic expression, functional performance and other features of in vivo human brain, including 85 d-CO [16, 29, 30]. Thus, 85 d-CO was chosen for establishing humanized ischemic stroke model in this study.

In addition to controlling the morphology and culture time of COs that were used for model preparation, we also explored the selection criteria for the size of COs. By measuring the size of 134 COs with 85 days culture time from five culture batches, and found the majority of them were more than 2.00 mm in diameter (2.38 ± 0.03 mm, $n = 98$, moderate size group), and a small part had a relatively smaller diameter (1.82 ± 0.01 mm, $n = 36$, small size group) (Fig. 3a, b). And, with introduction of OGD model (a classical in-vitro model of ischemic stroke), we further examined the injury degree of the COs from the two groups. As shown in Fig. 3c, d, the cell cytotoxicity of LDH release and cell apoptosis of Caspase 3 activity in moderate size group were about half the levels of those in small size group, indicating the different sensitivity to OGD injury for the two groups. In order to keep the experimental study as parallel as possible, COs in moderate and small size groups are suggested not to be used together for establishing model and drug efficacy testing. In our following study, 85 d-CO with diameter more than 2.00 mm was chosen for establishing humanized ischemic stroke model.

The time-effect relationship of COs-based humanized ischemic stroke model
Time-effect relationship is an important reference for establishing a novel research model. After separating 85 d-CO into 0 h (control group, under normal culture condition), 2 h, 4 h, 8 h, 12 h OGD exposure groups randomly, we explored the injury degree of COs (Fig. 4). H&E staining showed that the cell density in the tissue section of COs gradually decreased with the prolonged OGD exposure time (Fig. 4a). Compared with control group, the cell cytotoxicity of LDH release and cell apoptosis of Caspase 3 activity in 2 h, 4 h, 8 h, 12 h OGD exposure groups gradually increased with significant difference (Fig. 4b, c). Moreover, further examination for the expression of apoptotic cells by immunohistochemical staining Cleaved-Caspase 3, a marker of cell apoptosis, confirmed the result (Fig. 4d, e). The number of apoptotic cells gradually increased in the 0 h, 2 h, 4 h, 8 h and 12 h OGD exposure groups by quantification of Cleaved-Caspase 3^+ cells in each group (Fig. 4d, e). Taken together, the ischemic injury degree of COs is gradually increased along the OGD exposure time. The establishment of the time-effect relationship of COs-based humanized ischemic stroke model provides an experimental reference for selecting proper OGD exposure time or ischemic injury degree for drug testing.

The feasibility and validity of COs-based humanized ischemic stroke model in drug testing
Whether the model is feasible for drug testing is still a question due to it is the first study to focus on the preparation of COs-based humanized ischemic stroke model. In order to validate the sensitivity of the model for drug efficacy testing, the proven anti-apoptotic and pro-apoptotic compounds pan-Caspase inhibitor Z-VAD-FMK (20 μM) and Bcl-2 inhibitor navitoclax (0.5 μM) were given during OGD exposure to explore their effect on OGD injury (Fig. 5). As shown in Fig. 5a, b, treatment of Z-VAD-FMK or navitoclax significantly alleviated or aggravated ischemic injury respectively, as compared to vehicle control group under OGD condition. Besides, TUNEL staining for apoptotic cells and Nissl's staining for survival neurons further confirmed the anti-apoptotic effect of Z-VAD-FMK and pro-apoptotic effect of navitoclax in the humanized COs ischemic stroke model (Fig. 5c–f). As shown in Fig. 5c, d for TUNEL staining, compared to control group, the

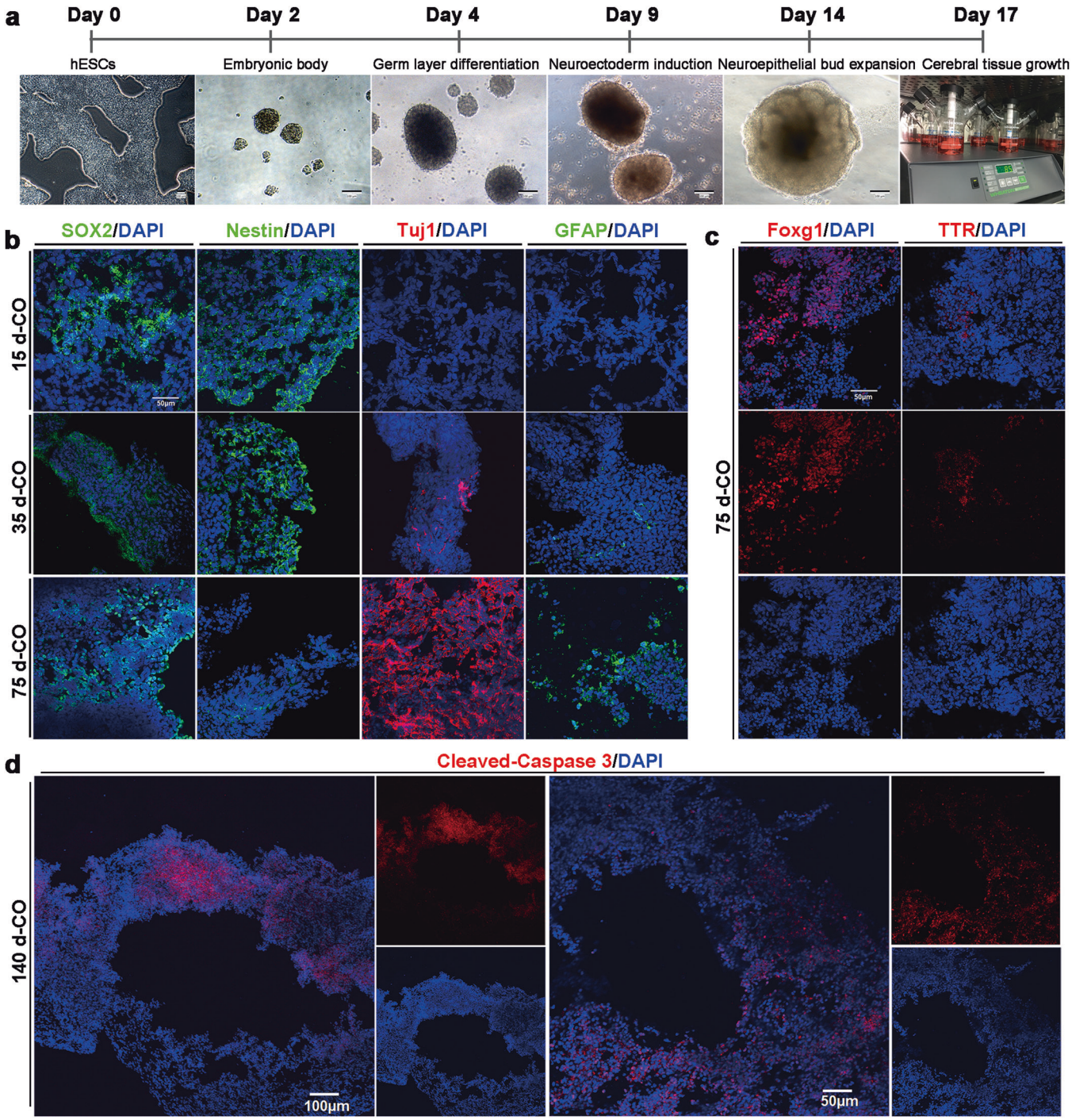

Fig. 1 The culture and identification of cerebral organoids (COs) at different culture time. a Schematic diagram for the culture process of COs. Human embryonic stem cells (hESCs, Day 0) underwent embryonic body formation (Day 2), germ layer differentiation (Day 4), neuroectoderm induction (Day 9) and neuroepithelial bud expansion (Day 14) in the low-attachment plate, and further developed into COs in the spinning bioreactor (after Day 17). **b** Immunostaining of COs at 15, 35 and 75 days with neural cell markers (SOX2, neural progenitor cell; Nestin, neural stem cell; Tuj-1, neuron; GFAP, astrocyte). **c** Immunostaining of COs at 75 days with brain region specific markers (Foxg1, forebrain; TTR, choroid plexus). **d** Immunostaining of COs at 140 days with apoptotic cell marker Cleaved-Caspase 3. DAPI labels nuclei (blue). All scale bars are as shown.

vehicle group had more expression of TUNEL positive cells. And Z-VAD-FMK treatment significantly decreased the expression of $TUNEL^+$ cells as compared to vehicle group, and showed no difference with control group; navitoclax treatment significantly increased the expression of $TUNEL^+$ cells as compared to vehicle group (Fig. 5c, d). Moreover, Nissl's staining for survival neurons showed the vehicle group had less expression of Nissl's positive cells than control group (Fig. 5e, f). And Z-VAD-FMK treatment significantly increased the expression of Nissl's positive cells as compared to vehicle group and had no difference with control group, and navitoclax treatment significantly decreased the expression of Nissl's positive cells as compared to vehicle group

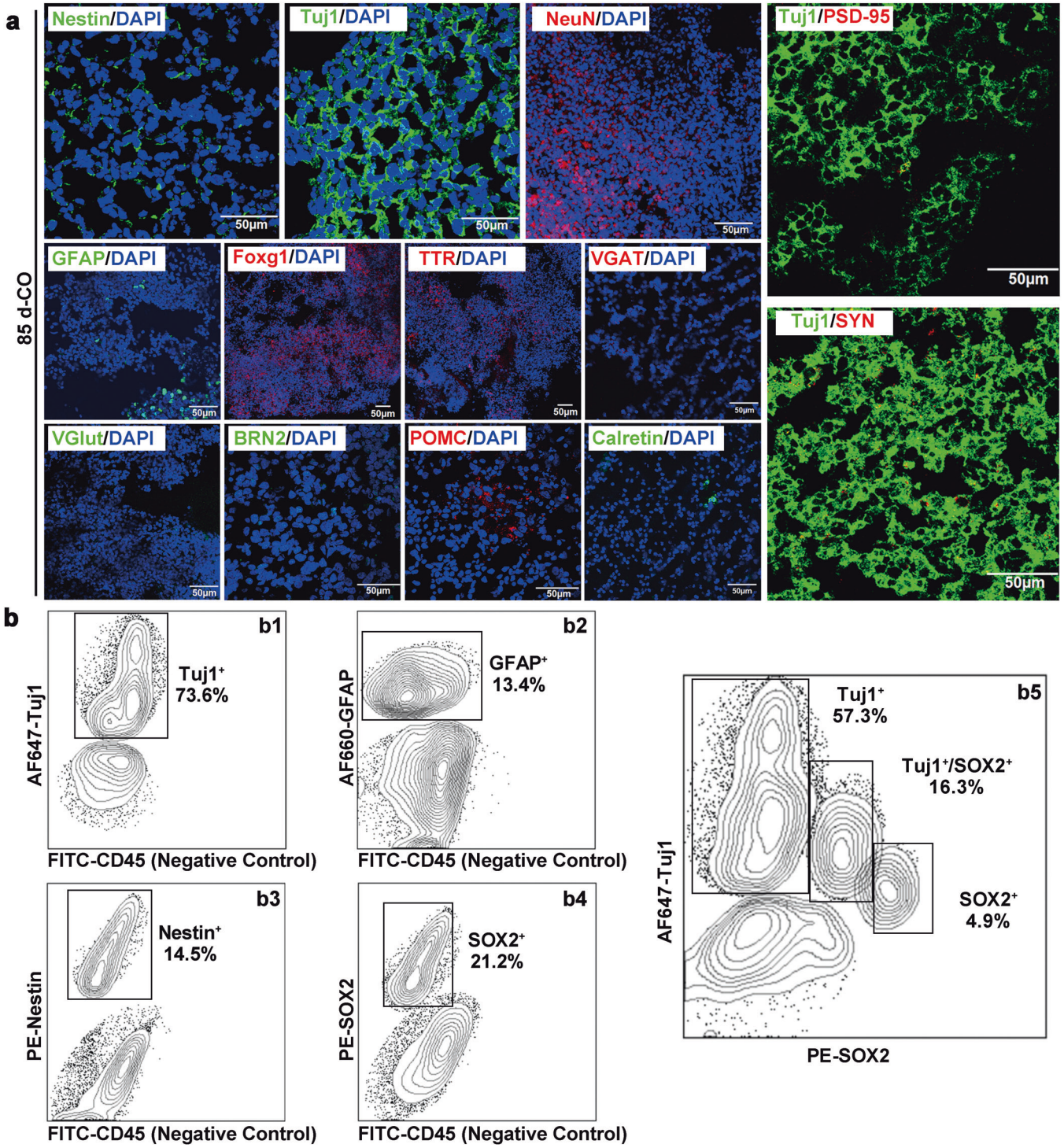

Fig. 2 The cell composition and cell ratio of COs at 85 days. a Immunostaining of COs at 85 days (85 d-CO) with neural stem cell marker Nestin, neuron marker Tuj1, mature neuron marker NeuN, astrocyte marker GFAP, forebrain marker Foxg1, choroid plexus marker TTR, inhibitory neuron marker VGAT, excitatory glutamatergic neuron marker VGlut, upper-layer neuron marker BRN2, peptidergic neuron marker POMC, interneuron marker Calretin, postsynaptic marker PSD-95 and presynaptic marker synaptophysin (SYN). DAPI labels nuclei (blue). All scale bars are as shown. **b** Representative image of Tuj1, GFAP, Nestin, SOX2 and Tuj1/SOX2 positive staining in 85 d-CO by flow cytometry. FITC-CD45 is used as negative control. Data are shown as mean ± SEM, and are representative of three independent experiments.

(Fig. 5e, f). Therefore, the COs-based humanized ischemic stroke model was sensitive to cerebral ischemic injury, and the ischemic injury can be changed with the treatment of anti-apoptotic or pro-apoptotic compounds, proving evidence for the feasibility of the model in drug efficacy testing. In addition to apoptosis, we explored the involved cell death manners in COs under OGD condition. As shown in Fig. 5g, there were positive expressions of Cleaved-Caspase 3^{+} apoptotic cells, Phosphor-RIP3^{+} necroptotic cells, LC3B^{+} autophagic cells and GPX4^{+} ferroptotic cells in the groups of control and vehicle groups, suggesting that there may be multiple cell death manners in COs induced by OGD injury.

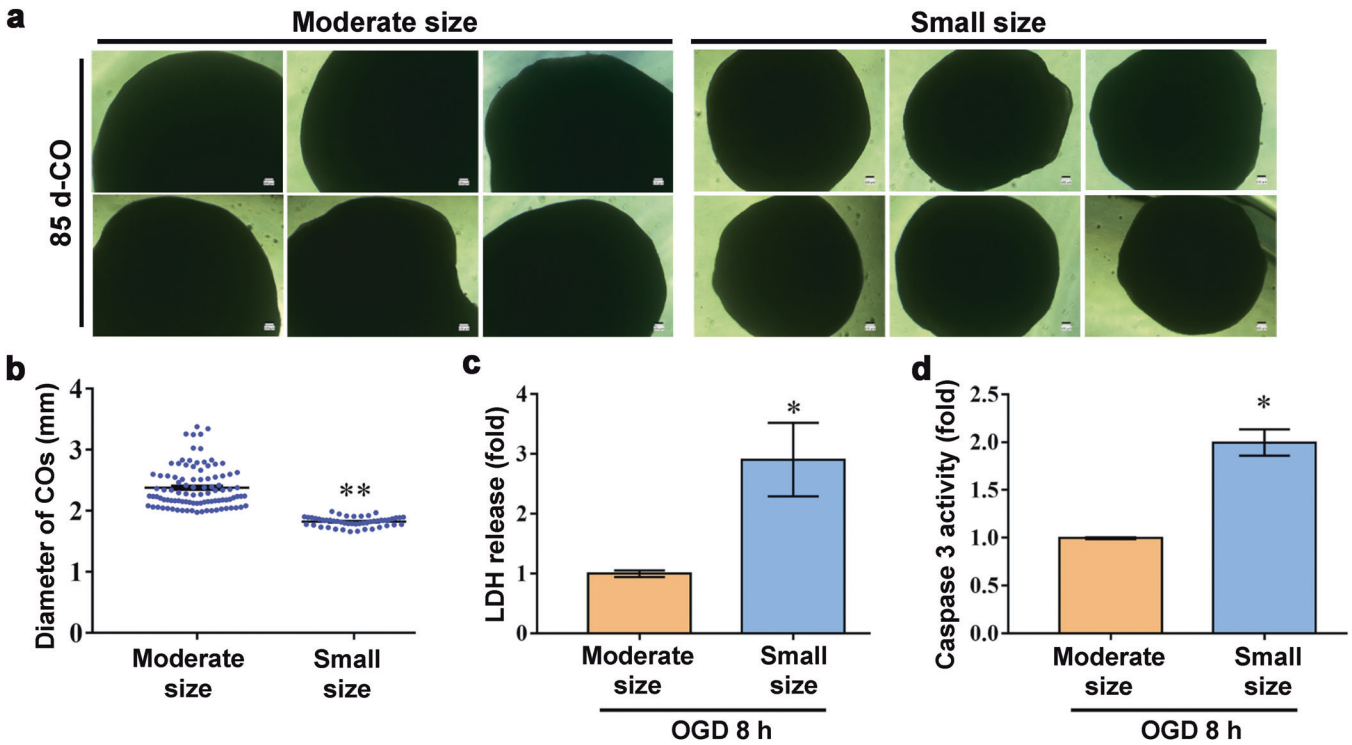

Fig. 3 The volume size of COs at 85 days. a The morphology and volume size of COs at 85 days in moderate and small size groups. **b** The diameter of COs at 85 days in moderate and small size groups (2.38 ± 0.03 vs. 1.82 ± 0.01 mm, $n = 98$ and 36 respectively). **c**, **d** The LDH release and Caspase 3 activity of COs at 85 days in moderate and small size groups after 8 h oxygen-glucose deprivation (OGD) exposure. Data are shown as mean ± SEM, and are representative of three independent experiments. $^{*}P < 0.05$, $^{**}P < 0.01$. All scale bars are as shown.

The sensitivity of COs-based humanized ischemic stroke model for neuroprotective compounds

The efficacies of four neuroprotective compounds (edaravone, butylphthalide, P7C3-A20, and ZL006) were tested in the humanized COs ischemic stroke model (Fig. 6a). According to the result of cell cytotoxicity of LDH release and cell apoptosis of Caspase 3 activity as shown in Fig. 6b, c, 10 μM edaravone, 10 μM butylphthalide, 10 μM P7C3-A20 and 10 μM ZL006 protected COs from ischemic injury under 8 h OGD condition. Therefore, the COs-based humanized ischemic stroke model can be also used for potential neuroprotective anti-stroke drug efficacy testing.

DISCUSSION

It is well-known that a good experimental model should be reliable and effective, which can not only produce consistent and reproducible results, but also predict clinical drug efficacy. At present, numerous in-vivo stroke research is mostly carried out in rodent animals, wherein stroke models in mouse and rat account for 27% and 66% of total in-vivo stroke model respectively [31]. And the OGD model is usually used as in-vitro stroke model to explore the effect of potential drug on the specific brain cell types, such as neurons, glial cells, etc., for efficacy evaluation and target validation at the molecular level [31]. Although almost all potential neuroprotective drugs have been studied for pharmacodynamics and mechanisms in the in-vitro and in-vivo models of stroke, all of them are still in the clinical translational research stage and few effective neuroprotective drug is available for stroke treatment so far [5]. Besides, although mouse or rat brain slices have been widely used as 3D model to study the role of different neural cell types in stroke, there are many disadvantages for the model, including additional mechanical injury during cutting, severed neural connections or loss of connections from distant brain areas to the area of interest, limited in-vitro culture time and so on [32–34]. The cultured COs not only have advantage in human species, but also show advantage in its 3D tissue structure, diverse cell types, detectable neural connectivity and projection that recapitulate features of in-vivo human brain. Therefore, we proposed whether it is possible to establish a humanized stroke model based on COs to provide a novel platform for anti-stroke drug efficacy testing and pathophysiological mechanism research. A most-recent study exposed COs to low-oxygen concentrations to model hypoxic injury [17], but the features of COs-based humanized ischemic stroke model in response to OGD damage and its application in testing anti-stroke drugs are still not explored. Thus, this study planned to establish an in-vitro humanized ischemic stroke model of OGD and explored its application in testing anti-stroke drugs (Fig. 7).

How to standardize the process of model preparation is the key problem to be solved for a new model. Due to the heterogeneity of COs in morphology and volume, we explored the selection criteria of COs for ischemic stroke model preparation. Firstly, we examined the cell type and composition of COs at different time. With the prolongation of culture time, expression of neural stem cells in COs gradually decreased and the terminally differentiated neurons and astrocytes gradually increased. And, there was the formation of forebrain and choroid plexus in 75 d-CO, indicating the successful generation of COs. Thus, we further prolonged the culture time of COs and employed 85 d-CO for model preparation, which had higher cell maturation degree and more expression of terminal differentiated neural cells than 75 d-CO. Although we found the formation of apoptotic cavity in tissue center of 140 d-CO, whether COs with longer culture time are suitable for OGD model preparation remains to be further verified. After measuring the diameter of 85 d-CO from different culture batch, we found that most COs were more than 2 mm in diameter and a small part of COs was <2 mm in diameter. Therefore, we grouped COs from same culture batch into moderate size group and small size group

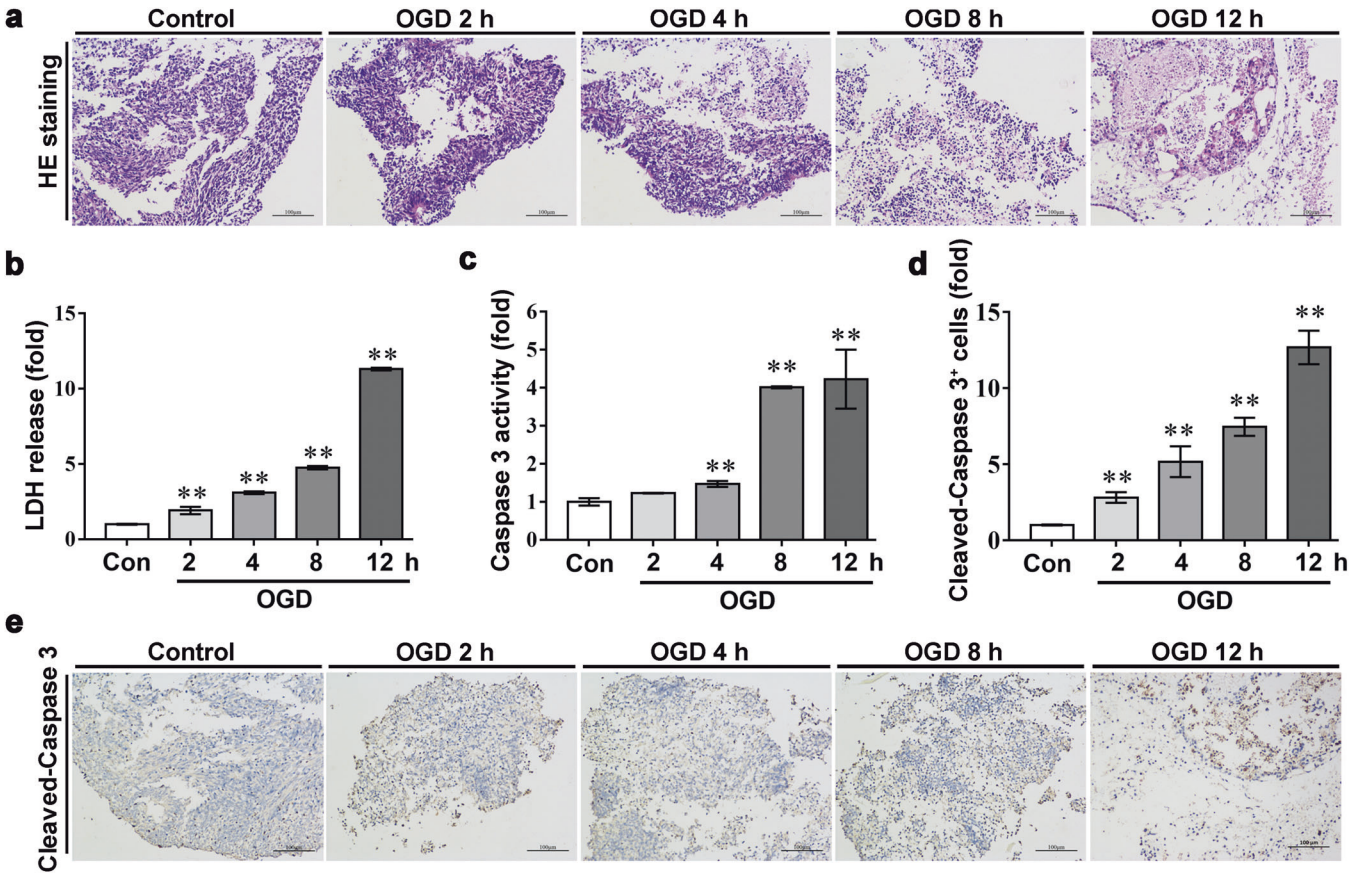

Fig. 4 The time-effect relationship of COs-based humanized ischemic stroke model. a The H&E staining of COs in 0 h, 2 h, 4 h, 8 h and 12 h OGD groups. **b**, **c** The LDH release and Caspase 3 activity of COs in 0 h, 2 h, 4 h, 8 h and 12 h OGD groups. **d**, **e** Immunostaining and quantification of Cleaved-Caspase 3 positive cells in COs of 0 h, 2 h, 4 h, 8 h and 12 h OGD groups. Data are shown as mean ± SEM, and are representative of three independent experiments. $^{**}P < 0.01$ vs. control. All scale bars are as shown.

respectively. Due to the different injury degree of COs between moderate and small size groups under OGD condition, we set the selection criteria of COs for establishing humanized stroke model, that is, in our study only employing COs with diameter more than 2 mm for the model preparation. As for a new research model, it is important to establish the time-effect relationship of the model. Thus, we explored the time-effect relationship of COs-based humanized stroke model, and found the ischemic injury degree of COs gradually aggravated with the extension of OGD time, providing an experimental reference for selecting the proper OGD time and ischemic injury degree during drug testing.

Ischemia would initiate the ischemic cascade which involves a series of biochemical events, including energy failure, ion imbalance and excitotoxicity, oxidative stress, cell death, complement system activation, initiation of the inflammation and immune response [35]. And increasing evidence proves that multiple cell death pathways are persistently present in the ischemic core and penumbral area, which play either beneficial, deleterious or dual roles in the progression of post-stroke brain damage [35]. The final death or survival state of ischemic injured cells is directly correlated with the prognosis after stroke. In order to validate the feasibility and applicability of the model for potential drug testing, this study introduced the proven anti-apoptotic and pro-apoptotic compounds pan-Caspase inhibitor Z-VAD-FMK and Bcl-2 inhibitor navitoclax as positive control to demonstrate that the model was sensitive to ischemic apoptotic injury and related treatment. In addition to apoptosis, this study provided early evidence that the cell death manners in COs induced by OGD injury may involve apoptosis, necroptosis, autophagy and ferroptosis. Future study needs to provide more evidence for the involved cell death manners of the model, and explore the vulnerability of different cell types and their sites inside the sphere of COs to different cell death manners under OGD condition.

Besides, four neuroprotective compounds (edaravone, butylphthalide, P7C3-A20 and ZL006) were introduced for further efficacy testing in the humanized COs ischemic stroke model. Thereinto, edaravone, a free radical scavenger, has been first approved in Japan by the Ministry of Health, Labour and Welfare for the treatment of ischemic stroke within 24 h of onset, and now is widely used for acute ischemic stroke within 24 h of onset following the guidelines for stroke management [36, 37]; butylphthalide is an anti-cerebral-ischemia drug which has been approved for ischemic stroke treatment by China Food and Drug Administration in 2002 [38]; P7C3-A20 has been demonstrated with neuroprotection in rodent model of ischemic stroke by our group [24] and of other disease models by several research groups [20]; ZL006, a small-molecular inhibitor of nNOS-PSD-95 interaction, has been demonstrated with neuroprotection in rodent model of ischemic stroke [39]. Here, we demonstrated that treatment of edaravone, butylphthalide, P7C3-A20 and ZL006 can protect COs from OGD injury. Therefore, COs-based humanized ischemic stroke model can be used for potential neuroprotectant efficacy testing.

Although this study explored the feasibility and applicability of the COs-based humanized ischemic stroke model in testing anti-stroke drugs, there are still many questions need to be answered. One of those major questions is lack of compounds as negative control to compare the difference of its efficacy in this model from that in clinical trial. It is known that numerous neuroprotective

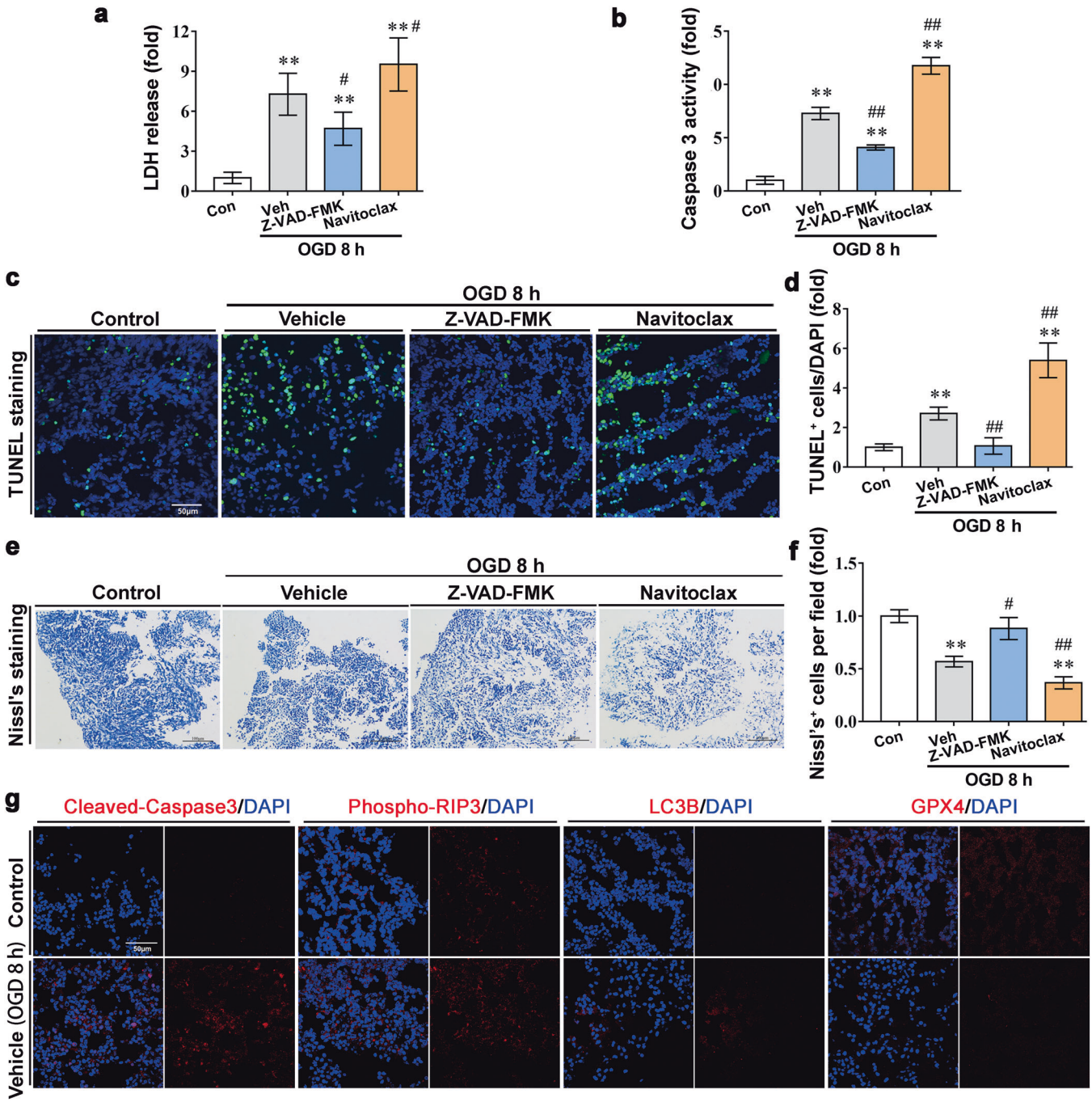

Fig. 5 The effect of anti-apoptotic and pro-apoptotic compounds in COs-based humanized ischemic stroke model. a The LDH release, **b** Caspase 3 activity, **c** the representative image of TUNEL staining, **d** quantification of the percentage of TUNEL^{+} cells, **e** the representative image of Nissl's staining and **f** quantification of the percentage of Nissl's cells per field in humanized COs ischemic stroke model under normal or under 8 h OGD condition with or without treatment of pan-Caspase inhibitor Z-VAD-FMK (20 μM) and Bcl-2 inhibitor navitoclax (0.5 μM). **g** Immunostaining for the expression of Cleaved-Caspase 3, Phopho-RIP3, LC3B and GPX4 in the control and vehicle groups of COs. DAPI labels nuclei (blue). Data are shown as mean ± SEM, and are representative of three independent experiments. $^{**}P < 0.01$ vs. control; $^{\#}P < 0.05$, $^{\#\#}P < 0.01$ vs. vehicle. All scale bars are as shown.

compounds have failed in clinical trials. However, until now, most of these compounds have failed due to safety or failure to show significant protection, and there are few reports on whether they failed due to differences in action targets caused by species difference between preclinical experiments and clinical trials. Future study needs to provide answer for the question. Besides, blood vessel unit, blood brain barrier and immune cells play crucial role in human ischemic stroke, but are absent in COs, which hamper the application of the model [40, 41]. Although many works have been done to resolve the problems in recent years [42, 43], there is still a long way to obtain an ideal COs containing vascular network, blood brain barrier and immune cells to achieve high-throughput screening in drug development. Thus, the culture method of COs needs to be further optimized to achieve better bioequivalence in the 3D spatial structure and cell tissue composition as compared to human brain.

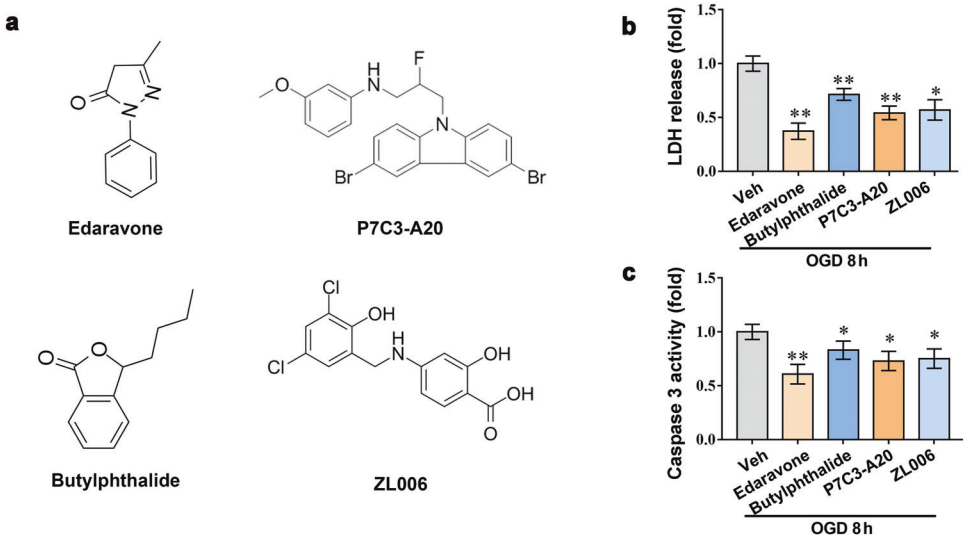

Fig. 6 The effect of neuroprotective compounds in COs-based humanized ischemic stroke model. a The chemical structure of edaravone, butylphthalide, P7C3-A20 and ZL006. **b** The LDH release and **c** Caspase 3 activity of COs under 8 h OGD condition with or without edaravone (10 μM), butylphthalide (10 μM), P7C3-A20 (10 μM) and ZL006 (10 μM) treatment. $^{*}P < 0.05$, $^{**}P < 0.01$ vs. vehicle group. Data are shown as mean ± SEM, and are representative of at least three independent experiments.

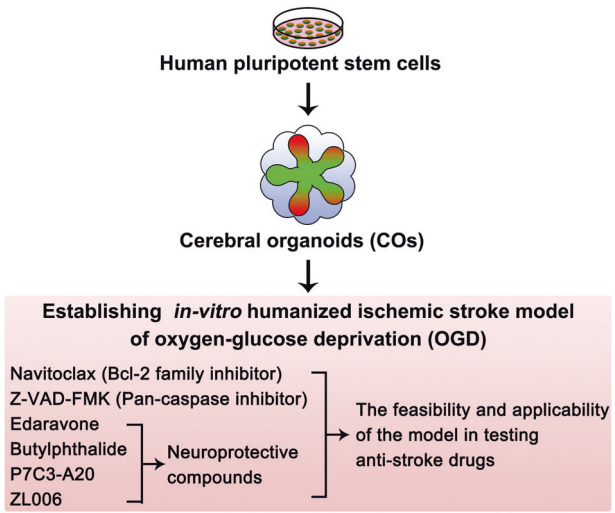

Fig. 7 Diagram showing the proposed application of COs-based humanized ischemic stroke model in studying anti-stroke drugs.

In summary, the study establishes a humanized ischemic stroke model based on COs, and validates the feasibility and applicability of the model in studying anti-stroke drugs, providing a new research platform for anti-stroke drug development.

ACKNOWLEDGEMENTS

This work was supported by grants from Medical Innovation Major Project (No. 16CXZ009), National Natural Science Foundation of China Major Project (No. 81730098), Youth Program of National Natural Science Foundation of China (No. 82003754 and No. 82104166), and Shanghai Science and Technology Commission Projects (No. 20YF1458400 and No. 21140901000).

AUTHOR CONTRIBUTIONS

SNW, ZW, and XYW designed and performed the majority of the experiments. SNW analyzed data and prepared the paper. XPZ carried out the culture of COs. TYX performed experimental design and data interpretation. CYM supervised the study, formulated the hypothesis, designed experiments, examined final manuscript and provided financial support for the study. All authors approved the final paper.

ADDITIONAL INFORMATION

Competing interests: The authors declare no competing interests.

REFERENCES

1. Campbell BCV, Khatri P. Stroke. Lancet. 2020;396:129–42.
2. Collaborators GBDLRoS, Feigin VL, Nguyen G, Cercy K, Johnson CO, Alam T, et al. Global, regional, and country-specific lifetime risks of stroke, 1990 and 2016. N Engl J Med. 2018;379:2429–37.
3. Hankey GJ. Stroke. Lancet. 2017;389:641–54.
4. Lozano R, Naghavi M, Foreman K, Lim S, Shibuya K, Aboyans V, et al. Global and regional mortality from 235 causes of death for 20 age groups in 1990 and 2010: a systematic analysis for the Global Burden of Disease Study 2010. Lancet. 2012;380:2095–128.
5. Chamorro A, Dirnagl U, Urra X, Planas AM. Neuroprotection in acute stroke: targeting excitotoxicity, oxidative and nitrosative stress, and inflammation. Lancet Neurol. 2016;15:869–81.
6. O'Collins VE, Macleod MR, Donnan GA, Horky LL, van der Worp BH, Howells DW. 1,026 experimental treatments in acute stroke. Ann Neurol. 2006;59:467–77.
7. Sommer CJ. Ischemic stroke: experimental models and reality. Acta Neuropathol. 2017;133:245–61.
8. Cook DJ, Tymianski M. Nonhuman primate models of stroke for translational neuroprotection research. Neurotherapeutics. 2012;9:371–9.
9. Tajiri N, Dailey T, Metcalf C, Mosley YI, Lau T, Staples M, et al. In vivo animal stroke models: a rationale for rodent and non-human primate models. Transl Stroke Res. 2013;4:308–21.
10. Wang Z, Wang SN, Xu TY, Hong C, Cheng MH, Zhu PX, et al. Cerebral organoids transplantation improves neurological motor function in rat brain injury. CNS Neurosci Ther. 2020;26:682–97.
11. Lancaster MA, Renner M, Martin CA, Wenzel D, Bicknell LS, Hurles ME, et al. Cerebral organoids model human brain development and microcephaly. Nature. 2013;501:373–9.
12. Lancaster MA, Knoblich JA. Generation of cerebral organoids from human pluripotent stem cells. Nat Protoc. 2014;9:2329–40.
13. Qian XY, Nguyen HN, Song MM, Hadiono C, Ogden SC, Hammack C, et al. Brain-region-specific organoids using mini-bioreactors for modeling ZIKV exposure. Cell. 2016;165:1238–54.
14. Arlotta P. Organoids required! A new path to understanding human brain development and disease. Nat Methods. 2018;15:27–9.
15. Wang Z, Wang SN, Xu TY, Miao ZW, Su DF, Miao CY. Organoid technology for brain and therapeutics research. CNS Neurosci Ther. 2017;23:771–8.
16. Luo C, Lancaster MA, Castanon R, Nery JR, Knoblich JA, Ecker JR. Cerebral organoids recapitulate epigenomic signatures of the human fetal brain. Cell Rep. 2016;17:3369–84.
17. Kim MS, Kim DH, Kang HK, Kook MG, Choi SW, Kang KS. Modeling of hypoxic brain injury through 3D human neural organoids. Cells. 2021;10:234.

18. Wang P, Miao CY. NAMPT as a Therapeutic target against stroke. Trends Pharmacol Sci. 2015;36:891–905.
19. Wang P, Shao BZ, Deng Z, Chen S, Yue Z, Miao CY. Autophagy in ischemic stroke. Prog Neurobiol. 2018;163-164:98–117.
20. Wang SN, Xu TY, Li WL, Miao CY. Targeting nicotinamide phosphoribosyltransferase as a potential therapeutic strategy to restore adult neurogenesis. CNS Neurosci Ther. 2016;22:431–9.
21. Zhao Y, Guan YF, Zhou XM, Li GQ, Li ZY, Zhou CC, et al. Regenerative neurogenesis after ischemic stroke promoted by nicotinamide phosphoribosyltransferase-nicotinamide adenine dinucleotide cascade. Stroke. 2015;46:1966–74.
22. Wang SN, Wang Z, Xu TY, Cheng MH, Li WL, Miao CY. Cerebral organoids repair ischemic stroke brain injury. Transl Stroke Res. 2020;11:983–1000.
23. Li W, Sun W, Zhang Y, Wei W, Ambasudhan R, Xia P, et al. Rapid induction and long-term self-renewal of primitive neural precursors from human embryonic stem cells by small molecule inhibitors. Proc Natl Acad Sci USA. 2011;108:8299–304.
24. Wang SN, Xu TY, Wang X, Guan YF, Zhang SL, Wang P, et al. Neuroprotective efficacy of an aminopropyl carbazole derivative P7C3-A20 in ischemic stroke. CNS Neurosci Ther. 2016;22:782–8.
25. Zhang SL, Li ZY, Wang DS, Xu TY, Fan MB, Cheng MH, et al. Aggravated ulcerative colitis caused by intestinal Metrnl deficiency is associated with reduced autophagy in epithelial cells. Acta Pharmacol Sin. 2020;41:763–70.
26. Bertolini JA, Favaro R, Zhu Y, Pagin M, Ngan CY, Wong CH, et al. Mapping the global chromatin connectivity network for Sox2 function in neural stem cell maintenance. Cell Stem Cell. 2019;24:462–476.e6.
27. Takahashi K, Yamanaka S. A decade of transcription factor-mediated reprogramming to pluripotency. Nat Rev Mol Cell Biol. 2016;17:183–93.
28. Mercurio S, Serra L, Motta A, Gesuita L, Sanchez-Arrones L, Inverardi F, et al. Sox2 acts in thalamic neurons to control the development of retina-thalamus-cortex connectivity. iScience. 2019;15:257–73.
29. Tanaka Y, Cakir B, Xiang Y, Sullivan GJ, Park IH. Synthetic analyses of single-cell transcriptomes from multiple brain organoids and fetal brain. Cell Rep. 2020;30:1682–1689.e3.
30. Dezonne RS, Sartore RC, Nascimento JM, Saia-Cereda VM, Romao LF, Alves-Leon SV, et al. Derivation of functional human astrocytes from cerebral organoids. Sci Rep. 2017;7:45091.
31. Neuhaus AA, Couch Y, Hadley G, Buchan AM. Neuroprotection in stroke: the importance of collaboration and reproducibility. Brain. 2017;140:2079–92.
32. Van Hoeymissen E, Philippaert K, Vennekens R, Vriens J, Held K. Horizontal hippocampal slices of the mouse brain. J Vis Exp. 2020;163:e61753.
33. Voss LJ. A systematic exploration of local network state space in neocortical mouse brain slices. Brain Res. 2022;1779:147784.
34. Hohmann U, Dehghani F, Hohmann T. Assessment of neuronal damage in brain slice cultures using machine learning based on spatial features. Front Neurosci. 2021;15:740178.
35. Sekerdag E, Solaroglu I, Gursoy-Ozdemir Y. Cell death mechanisms in stroke and novel molecular and cellular treatment options. Curr Neuropharmacol. 2018;16:1396–415.
36. Sun YY, Li Y, Wali B, Li Y, Lee J, Heinmiller A, et al. Prophylactic edaravone prevents transient hypoxic-ischemic brain injury: implications for perioperative neuroprotection. Stroke. 2015;46:1947–55.
37. Wang XX, Wang F, Mao GH, Wu JC, Li M, Han R, et al. NADPH is superior to NADH or edaravone in ameliorating metabolic disturbance and brain injury in ischemic stroke. Acta Pharmacol Sin. 2022;43:529–40.
38. Li F, Ma Q, Zhao H, Wang R, Tao Z, Fan Z, et al. L-3-n-Butylphthalide reduces ischemic stroke injury and increases M2 microglial polarization. Metab Brain Dis. 2018;33:1995–2003.
39. Zhou L, Li F, Xu HB, Luo CX, Wu HY, Zhu MM, et al. Treatment of cerebral ischemia by disrupting ischemia-induced interaction of nNOS with PSD-95. Nat Med. 2010;16:1439–43.
40. Yang C, Hawkins KE, Doré S, Candelario-Jalil E. Neuroinflammatory mechanisms of blood-brain barrier damage in ischemic stroke. Am J Physiol Cell Physiol. 2019;316:C135–53.
41. Wang HY, Ye JR, Cui LY, Chu SF, Chen NH. Regulatory T cells in ischemic stroke. Acta Pharmacol Sin. 2022;43:1–9.
42. Mansour AA, Goncalves JT, Bloyd CW, Li H, Fernandes S, Quang D, et al. An in vivo model of functional and vascularized human brain organoids. Nat Biotechnol. 2018;36:432–41.
43. Tang XY, Wu S, Wang D, Chu C, Hong Y, Tao M, et al. Human organoids in basic research and clinical applications. Signal Transduct Target Ther. 2022;7:168.

Springer Nature or its licensor holds exclusive rights to this article under a publishing agreement with the author(s) or other rightsholder(s); author self-archiving of the accepted manuscript version of this article is solely governed by the terms of such publishing agreement and applicable law.